

Inverter sizing of grid-connected photovoltaic systems in the light of local solar resource distribution characteristics and temperature

Bruno Burger^{a,1}, Ricardo R  ther^{b,*}

^a *Fraunhofer-Institute for Solar Energy Systems ISE, Department of Electrical Energy Systems, Heidenhofstr. 2, 79110 Freiburg, Germany*

^b *LABSOLAR—Laborat  rio de Energia Solar, LabEEE—Laborat  rio de Efici  ncia Energ  tica em Edifica  es, Universidade Federal de Santa Catarina/UFSC, Caixa Postal 476, Florian  polis—SC 88040-900, Brazil*

Received 20 December 2004; received in revised form 15 August 2005; accepted 18 August 2005

Available online 10 October 2005

Communicated by: Associate Editor Aaron Sanchez-Juarez

Abstract

Inverter sizing strategies for grid-connected photovoltaic (PV) systems often do not take into account site-dependent peculiarities of ambient temperature, inverter operating temperature and solar irradiation distribution characteristics. The operating temperature affects PV modules and inverters in different ways and PV systems will hardly ever have a DC output equal to or above their STC-rated nominal power. Inverters are usually sized with a nominal AC output power some 30% (sometimes even more) below the PV array nominal power. In this paper, we show that this practice might lead to considerable energy losses, especially in the case of PV technologies with high temperature coefficients of power operating at sites with cold climates and of PV technologies with low temperature coefficients of power operating at sites with warm climates and an energy distribution of sunlight shifted to higher irradiation levels. In energy markets where PV kWh's are paid premium tariffs, like in Germany, energy yield optimization might result in a favorable payback of the extra capital invested in a larger inverter.

This paper discusses how the time resolution of solar radiation data influences the correct sizing of PV plants.

We demonstrate that using instant (10 s) irradiation values instead of average hourly irradiation values leads to considerable differences in optimum inverter sizing. When calculating inverter yearly efficiency values using both, hourly averages and 1-min averages, we can show that with increased time resolution of solar irradiation data there are higher calculated losses due to inverter undersizing. This reveals that hourly averages hide important irradiation peaks that need to be considered.

We performed these calculations for data sets from pyranometer readings from Freiburg (48°N, Germany) and Florian  polis (27°S, Brazil) to further show the peculiarities of the site-dependent distribution of irradiation levels and its effects on inverter sizing.

   2005 Elsevier Ltd. All rights reserved.

Keywords: Inverter sizing; Grid-connected PV systems

* Corresponding author. Tel.: +55 48 331 5174; fax: +55 48 331 7615.

E-mail addresses: bruno.burger@ise.fraunhofer.de (B. Burger), ruther@mbox1.ufsc.br (R. R  ther).

¹ Tel.: +49 761 4588 5237; fax: +49 761 4588 9237.

Nomenclature

Abbreviations

| | |
|------|----------------------------------|
| PV | photovoltaic |
| STC | standard test conditions |
| c-Si | crystalline silicon |
| a-Si | amorphous silicon |
| CdTe | cadmium telluride |
| BIPV | building-integrated photovoltaic |
| Inv | inverter |

Subscripts

| | |
|-----|--------------|
| PV | photovoltaic |
| Inv | inverter |

MPP maximum power point

Symbols

| | |
|-------------------|--|
| P_{PV} | solar generator nominal power under STC (Wp) |
| η_{MPP} | MPP tracking efficiency (%) |
| η_{Inv} | inverter efficiency (%) |
| P_{Inv,AC_nom} | inverter AC nominal power (W) |
| | DC energy yield (kW h/kWp) |
| G | global horizontal irradiance (W/m ²) |

1. Introduction

Grid-connected applications are the fastest growing segment of the photovoltaic (PV) market with premium feed-in tariffs available in many countries (Perezagua et al., 2004). In many situations optimizing the PV array energy yield will justify the extra cost that might be incurred by this optimization (Baumgartner et al., 2004) and inverter sizing might be an interesting design aspect to look into. System design recommendations for grid-connected PV installations usually lead to inverters with a nominal power considerably smaller than the PV array's nominal power. Because of the perceived notion that PV systems will hardly ever have a DC output equal to or above their STC²-rated nominal power P_{PV} , inverters are often sized with a nominal power some 30% (sometimes even more) below the PV array nominal power (Keller and Affolter, 1995; Jantsch, 1996; Zilles and Oliveira, 2001; Pregelj et al., 2002; van der Borg and Burgers, 2003; Woyte et al., 2003). Furthermore, inverter technology has evolved considerably in recent years, with improved efficiencies especially at partial loads. In addition today's PV module nominal power tolerances have improved to $\pm 2.5\%$ (Photon, 2004) compared to previous $\pm 10\%$ (Zilles et al., 1998; Hecktheuer et al., 2001). In practice, recent measurements on 150 new mono- and multicrystalline PV modules, made at the Fraunhofer-Institute for Solar Energy Systems ISE (Kiefer, 2004), have resulted in a mean

–2.6% power deviation from STC with only a few PV modules showing deviations below –10% (see Fig. 1).

Especially for the market-dominant crystalline silicon (c-Si) PV technology, which presents a strong negative temperature coefficient of power, the high irradiation levels that lead to maximum output are associated with high cell operating temperatures, which usually prevent the PV array to reach its nominal DC power. This rationale has led to a rule of thumb, by which inverter nominal power can be designed lower than the PV array nominal DC power. This practice might lead to considerable energy losses, as this paper shows, especially in the case of PV technologies with small temperature coefficients of power like thin film amorphous silicon (a-Si) and cadmium telluride (CdTe) operating at sites with warm climates, high incidence of clear skies and an energy distribution of sunlight shifted to higher irradiation levels (R  ther et al., 2004). In the particular case of a-Si, it has recently been shown that different device designs (single vs. tandem junctions) and alloy characteristics (a-Si:H vs. a-SiGe:H) lead to different temperature coefficients of power (Shima et al., 2005) with a nonlinear, stronger effect at higher operating temperatures. It also has been shown that a-Si output performance stabilizes at different levels depending on the particular site prevailing temperature conditions with higher stabilized performance levels at sites with a year-round higher temperature (R  ther et al., 2003).

State-of-the-art inverters reach peak efficiencies of 95–97% at partial loads of 30–50% of nominal power and somewhat reduced efficiencies at full load. Undersized inverters might therefore operate

² STC = standard testing conditions (operating cell temperature = 25 °C; irradiation level = 1000 W/m²; incident spectrum = AM 1.5).

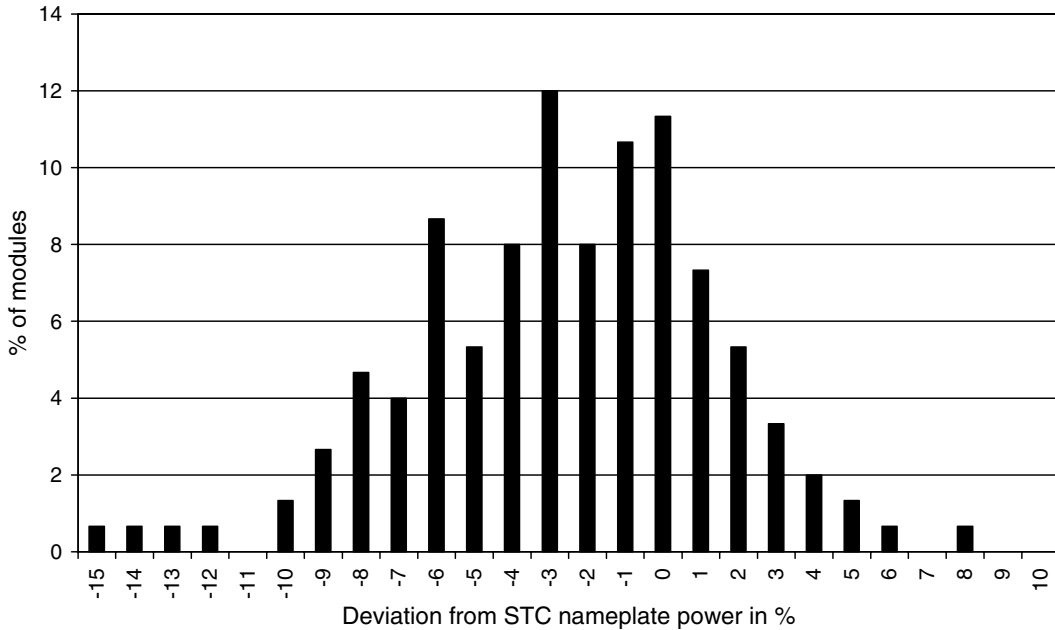


Fig. 1. Deviation from STC nameplate power of 150 new mono- and multicrystalline PV modules measured between July and December 2004 at ISE. Mean deviation = -2.6% (Kiefer, 2004).

closer to full capacity (and therefore below maximum performance levels) most of the time depending on the site distribution of irradiation levels. Furthermore, because undersized inverters will operate at full load more often, they will reach operating temperatures that might trigger temperature-

reducing features of their algorithms, leading to further energy losses. Fig. 2 shows the total efficiency (H  berlin et al., 2005) of an inverter vs. percentage of nominal capacity curve. The total efficiency is the product of the MPP tracking efficiency η_{MPP} and the inverter efficiency η_{Inv} . It therefore includes the

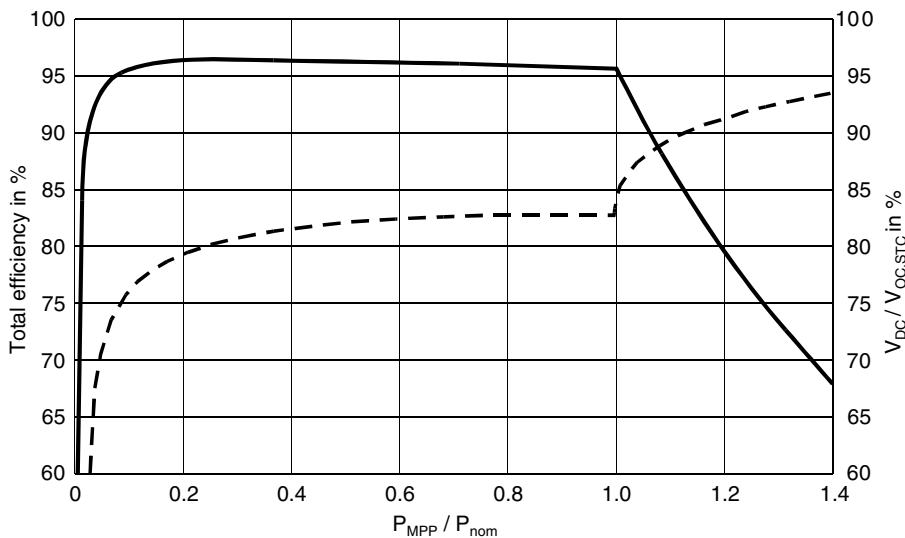


Fig. 2. Typical inverter total efficiency curve (solid line) and DC operating voltage (dashed line) as a function of loading (percentage of nominal DC power), including power limitation losses for input power levels above the inverter nominal power (Sunways, 2004). The inverter’s maximum efficiency lies at 30% of its nominal power.

power limitation losses due to overloading of the inverter (Sunways, 2004). This figure shows that when overloaded, inverters will limit the output power to nominal power. This is done by increasing the DC voltage from maximum power point voltage towards open circuit voltage. Above nominal power input, there is a hyperbolic decline in total efficiency. Many inverters are not able to work at nominal power conditions for prolonged periods of time because they warm up very fast. The inverters' control strategy is designed to limit the inverter's temperature, by shifting the PV array operating voltage from its maximum power point towards open circuit conditions. This situation might also be triggered by high ambient temperatures, which are usually associated with high irradiation levels. For one particular inverter manufacturer (Wurth, 2003) internal operating temperatures of 65 °C will trigger the temperature (power) reduction feature, limiting peak power to 70% of nominal; at 70–75 °C the output power will be reduced to 30% of nominal and above 75 °C the inverter will be disconnected from the grid. Overloading inverters might also reduce their operating life due to electronic component stress. The relatively small additional cost of a larger inverter to reduce component stress can often be justified economically by the consequent increase in the inverter's mean time to failure.

These aspects are analyzed and discussed in this paper regarding the influence of the time resolution of the irradiation data set used to determine a par-

ticular site irradiation distribution. Most of the available irradiation data at individual sites is measured as hourly averages, which leads to filtering of irradiation peak values that might result in inaccurate performance estimations.

2. Irradiation data sampling rate

We have studied the distribution of the incoming solar radiation at Fraunhofer-Institute of Solar Energy (ISE) in Freiburg (48°N, Germany, with typical yearly global horizontal radiation ~ 1150 kW h/m²) and at the Solar Energy Research Laboratory (LABSOLAR), Florianopolis (27°S, Brazil, with typical yearly global horizontal radiation ~ 1550 kW h/m²) based on global horizontal irradiation data, measured by calibrated clear glass pyranometers. At ISE we have measured instant (10 s) data and calculated 1-min and hourly averages. At LABSOLAR, we have measured 1-min averaged data and calculated hourly averages.

Fig. 3 shows the energy distribution of the incoming solar radiation for Freiburg, using instant values, 1-min averages and hourly averages. Each bar represents the percentage of the energy content in intervals of 50 W/m².

Fig. 3 and Table 1 demonstrate that while over 63% of daytime hours have instant radiation levels ≤ 300 W/m², the corresponding energy content represents only some 20% of the total incident energy. Looking at the high end of the radiation level shows

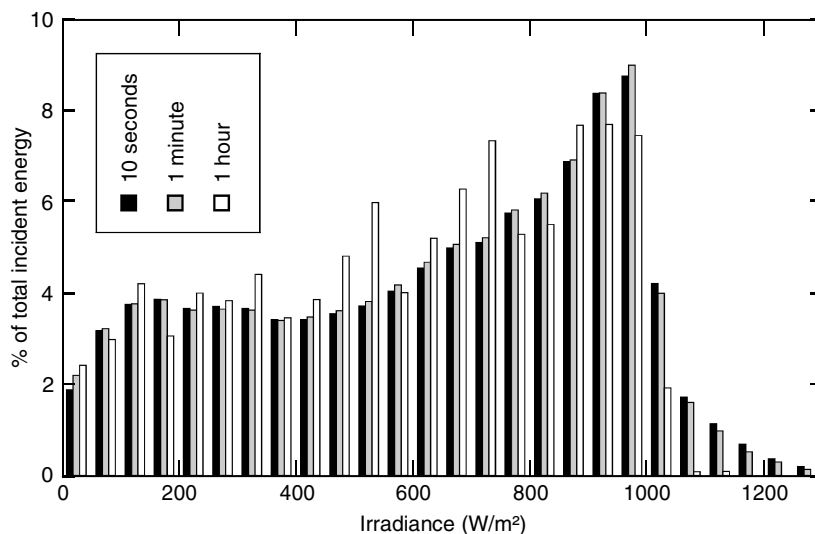


Fig. 3. Energy content distribution in percentage of total incident energy using instant (10 s) values (left bars), 1-min averages (central bars) and hourly averages (right bars) for irradiance intervals of 50 W/m² at the Freiburg site.

Table 1

Solar energy distribution in terms of percentage of daytime hours and percentage of energy content for different irradiance ranges in Freiburg, Germany and Florianopolis, Brazil, using different data sampling time resolutions

| Irradiance range G (W/m^2) | Freiburg | | | | | | Florianopolis | | | |
|--|-----------------------|--------------|-------|----------------------------|--------------|-------|-----------------------|-------|----------------------------|-------|
| | Percentage of daytime | | | Percentage of total energy | | | Percentage of daytime | | Percentage of total energy | |
| | 10 s | 1 min | 1 h | 10 s | 1 min | 1 h | 1 min | 1 h | 1 min | 1 h |
| $G \leq 300$ | 63.45 | 63.85 | 63.32 | 19.39 | 20.17 | 20.48 | 50.65 | 52.72 | 14.48 | 14.82 |
| $G \leq 700$ | 83.04 | 83.37 | 85.64 | 49.52 | 51.68 | 58.25 | 75.72 | 78.54 | 44.78 | 49.79 |
| $750 < G < 950$ | 11.80 | 11.74 | 11.72 | 31.18 | 32.36 | 33.39 | 17.80 | 18.16 | 36.08 | 39.05 |
| $G \geq 1000$ | 5.15 | 4.89 | 2.64 | 16.67 | 16.50 | 9.01 | 9.16 | 6.47 | 23.40 | 10.73 |
| $900 < G < 1500$ | 10.31 | 9.98 | 7.20 | 31.47 | 31.72 | 23.24 | 15.96 | 12.65 | 38.76 | 25.66 |

that only some 5% of the daytime hours have instant radiation levels $\geq 1000 \text{ W}/\text{m}^2$ but the corresponding energy content is over 16%.

Hourly averages tend to smooth out maxima, resulting in a distribution profile which is quite different from the ones resulting from instant values. The energy content of hourly averages appears to shift to lower irradiation levels. While still over 63% of daytime hours have radiation levels $\leq 300 \text{ W}/\text{m}^2$ with a corresponding energy content of some 20% of the total incident energy, less than 3% of daytime hours have radiation levels $\geq 1000 \text{ W}/\text{m}^2$, corresponding to only 9% of the incident energy. These results are considerably different from what is seen for 10 s time resolutions, demonstrating that the commonly used hourly averages hide important information and are not representative of the real solar resource distribution profiles. It is thus clear that the real energy content at these higher irradiation levels is underestimated when hourly averages are used. These results show that in fact system designs with $P_{\text{PV}}/P_{\text{Inv}} > 1$ will lead to inverters operating close to or above their nominal DC input levels more often than would be assumed by the use of (more commonly available) hourly averages of solar radiation data. This effect will be more pronounced for the thin-film a-Si PV technology due to the small net effect of temperature on PV device performance at the associated high irradiation levels.

Fig. 3 also demonstrates that 1-min and 10-s results are very similar to each other and do not justify the extra file sizes and computation times incurred by the instant values as compared to the 1-min averages. It can also be noticed that there is no distinction among the three sampling intervals at low irradiation levels. On the other hand, an

experimental/measurement artifact misleadingly demonstrates that hourly averages have higher energy content at irradiation levels above $300 \text{ W}/\text{m}^2$ and below $900 \text{ W}/\text{m}^2$.

Figs. 4 and 5 show, respectively, for a clear and a cloudy day, the different curve shapes of solar radiation data shown as instant (10 s) and mean hourly values at the Freiburg site.

Looking at the solar energy resource distribution at the Florianopolis site, respectively, at 1-min and hourly averages, Fig. 6 and Table 1 show that while over 50% of the daytime hours have radiation levels $\leq 300 \text{ W}/\text{m}^2$, the corresponding energy content represents less than 15% of the total incident energy. At these low-light levels, there is not much difference between the two different time resolutions. Considerable differences emerge when looking at the high end of the radiation level distribution. Using 1-min averages results in some 9% of the daytime hours with radiation levels $\geq 1000 \text{ W}/\text{m}^2$ and a corresponding energy content of some 23%. Using hourly averages results in around 6% of daytime hours with radiation levels $\geq 1000 \text{ W}/\text{m}^2$, and a corresponding energy content below 11%.

Comparing results from the two sites reveals that the experimental artifact introduced by hourly averages is much more pronounced for the sunny site Florianopolis, where undersizing of inverters will also lead to higher losses due to higher operating temperatures. We have recently shown DC performance ratios of over 90% (R  ther et al., 2004) for a 2 kWp thin-film a-Si PV system operating at the Florianopolis site since 1997 (R  ther and Dacoregio, 2000) with PV module temperatures reaching over $70 \text{ }^\circ\text{C}$. Under these conditions undersized inverters will operate at lower efficiency levels as shown in the right-hand side of Fig. 2.

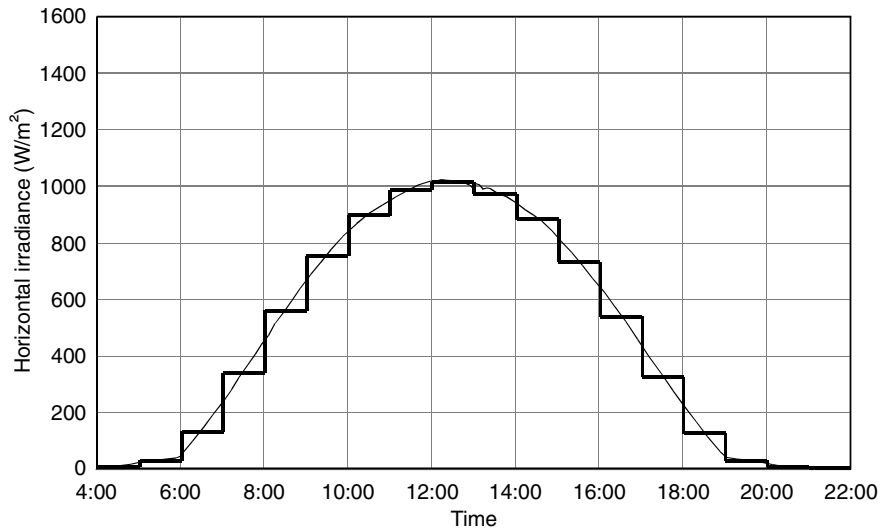


Fig. 4. Horizontal irradiance during a typical sunny day in Freiburg, with instant (10 s) values shown as a smooth continuous curve (thin) and mean hourly values shown as a stepped curve (thick).

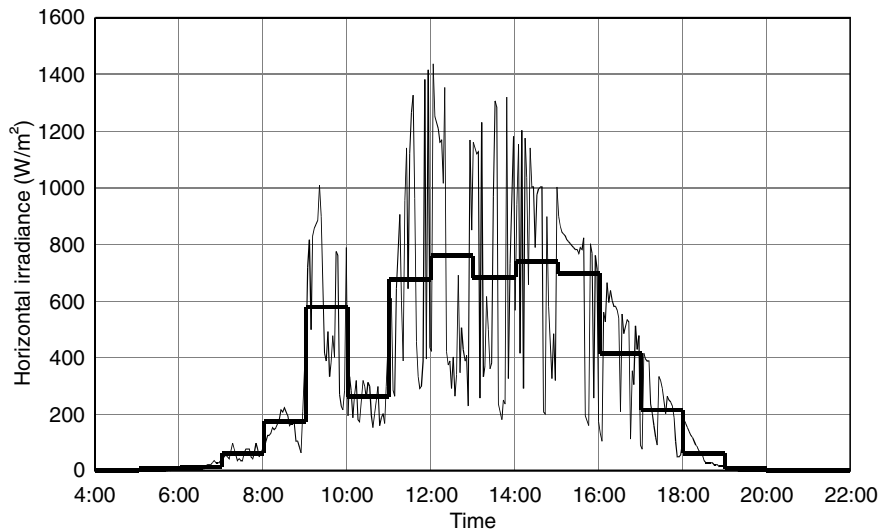


Fig. 5. Horizontal irradiance during a typical cloudy day in Freiburg, with instant (10 s) values shown as a jagged curve (thin) and mean hourly values shown as a stepped curve (thick).

3. Inverter yearly efficiencies and losses

Based on the irradiation data sampling rate and on the inverter typical efficiency profile as presented in Fig. 2, we have calculated inverter yearly efficiencies and losses due to power limitation.

Fig. 7 shows inverter yearly efficiency (%) curves, including power limitation losses for the Freiburg site as a function of the relation between the solar generator nominal DC power rating (P_{PV} in Wp) and the inverter AC nominal rating (ratio $P_{PV}/P_{Inv,AC_nom}$).

The solid line corresponds to instant (10 s) data, the dashed line corresponds to mean minute values, and the dotted line corresponds to mean hourly values. It can be noticed that hourly averages of solar radiation data lead to undersized inverters with respect to the PV generator DC nominal power.

Fig. 8 shows the inverter yearly efficiency (%) curves, including power limitation losses, for the Florianopolis site. The dashed line corresponds to mean minute values, and dotted line corresponds to mean hourly values. It can be seen that if

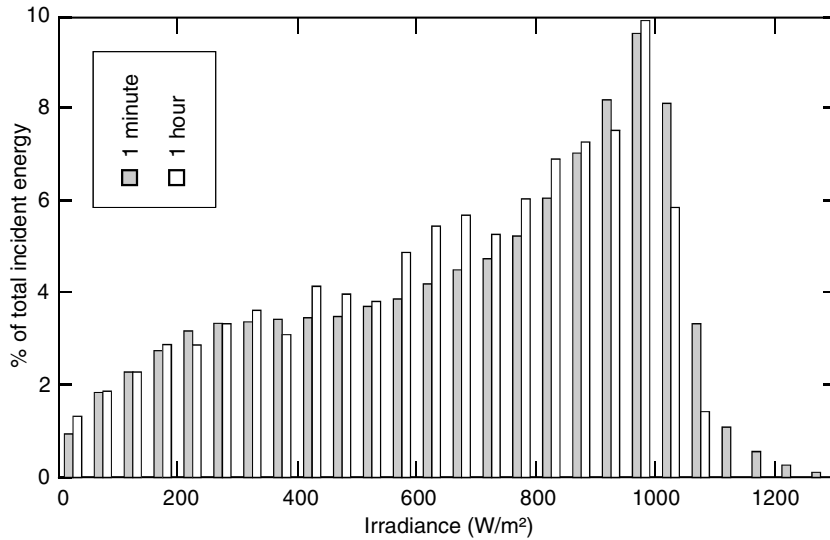


Fig. 6. Energy content distribution in percentage of total incident energy of 1-min average values (left bar) and hourly average values (right bar) for irradiance intervals of 50 W/m^2 at the Florianopolis site.

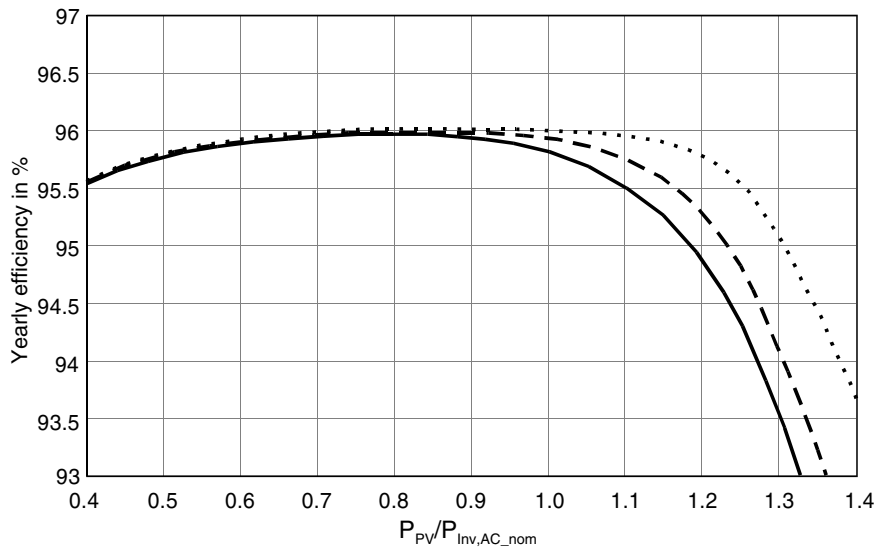


Fig. 7. Inverter yearly efficiency (in %), including power limitation losses, at the Freiburg site. The solid line corresponds to instant (10 s) values; the dashed line corresponds to mean minute values and the dotted line corresponds to mean hourly values of the solar radiation.

$P_{PV}/P_{Inv,AC,nom}$ is set above 1.1, hourly averages tend to overestimate efficiency and underestimate losses, demonstrating the experimental artifact induced by the use of the lower time resolution radiation data.

Fig. 9 shows the behavior of two identical $650 \text{ W}_{AC,nom}$ inverters (Inv1 and Inv2) for a typical, mostly clear sky, summer day in Florianopolis. The inverters are connected to two PV arrays with DC ratings of 640 Wp (Inv1) and 768 Wp (Inv2) with

identical amorphous silicon PV modules. It is clear that from around 10:30 to 14:30 some of the 768 Wp nominal DC power available at the inverter Inv2's input could not be processed due to the inverter's power limitation. The AC output of inverter Inv2 is normalized to the DC input of inverter Inv1 (normalization factor = $640/768$). The figure also shows both inverters temperatures with time. It can be seen that from 9:00, and more noticeable in the afternoon, inverter Inv2 reaches higher

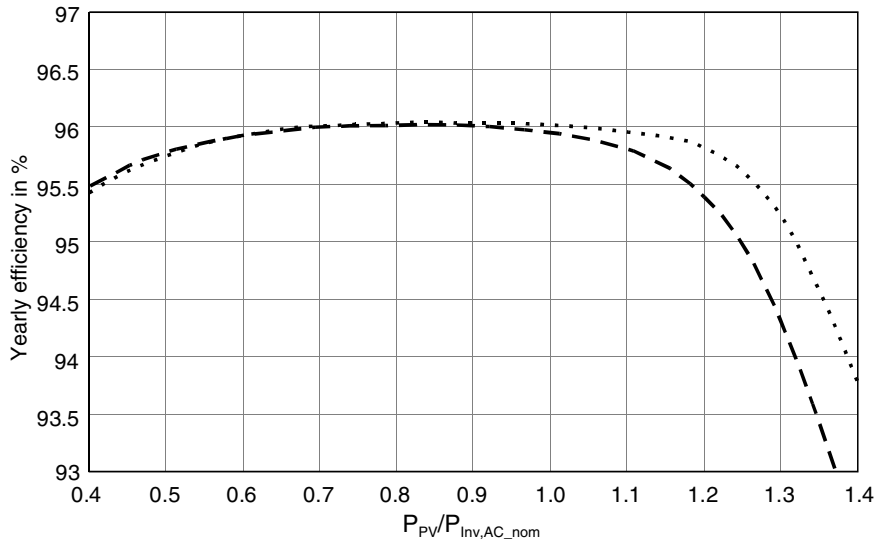


Fig. 8. Inverter yearly efficiency (in %), including power limitation losses, at the Florianopolis site. The dashed line corresponds to mean minute values and the dotted line corresponds to mean hourly values of the solar radiation.

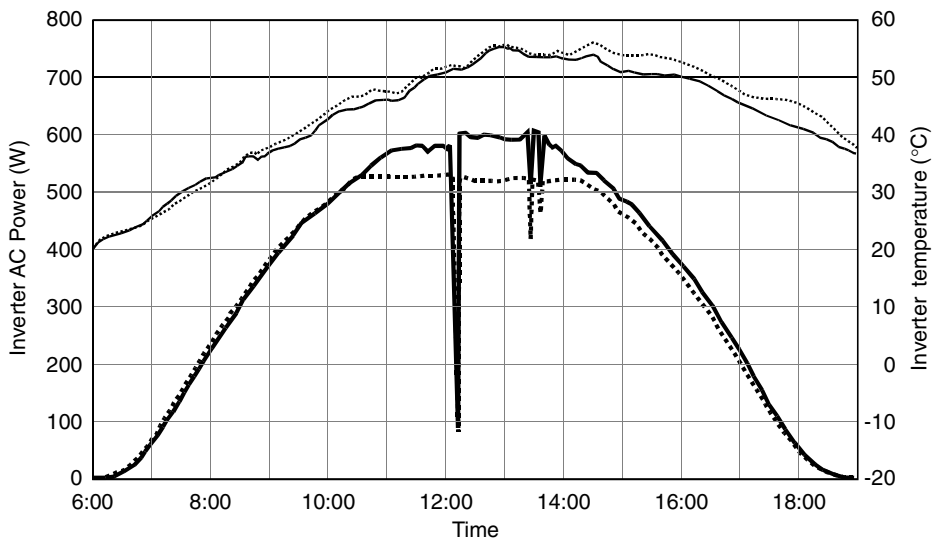


Fig. 9. AC output power of two identical 650 W AC inverters, connected to PV arrays with 640 Wp (Inv1; thick, solid curve) and 768 Wp (Inv2; thick, dotted curve) nominal DC ratings, operating in Florianopolis during a typical clear sky day. The AC output power of Inv2 is normalized by the factor 640/768, which is the ratio of the nominal DC ratings. The two thin curves correspond to the inverters' temperatures (solid curve = Inv1 and dotted curve = Inv2).

temperatures than inverter Inv1. This effect is seen in the normalized Inv2 curve in Fig. 9 (starting from around 14:30) where the normalized Inv2's output is slightly smaller than the output of Inv1. The amount of energy wasted over a full year under these conditions and an economic analysis of the tradeoffs of inverter sizing vs. inverter costs will be quantified when enough operational data becomes

available and will be presented in a further publication.

4. Solar energy resource and PV annual DC energy yield

Figs. 10 and 11 show, respectively, for Freiburg and Florianopolis, the total annual incoming solar

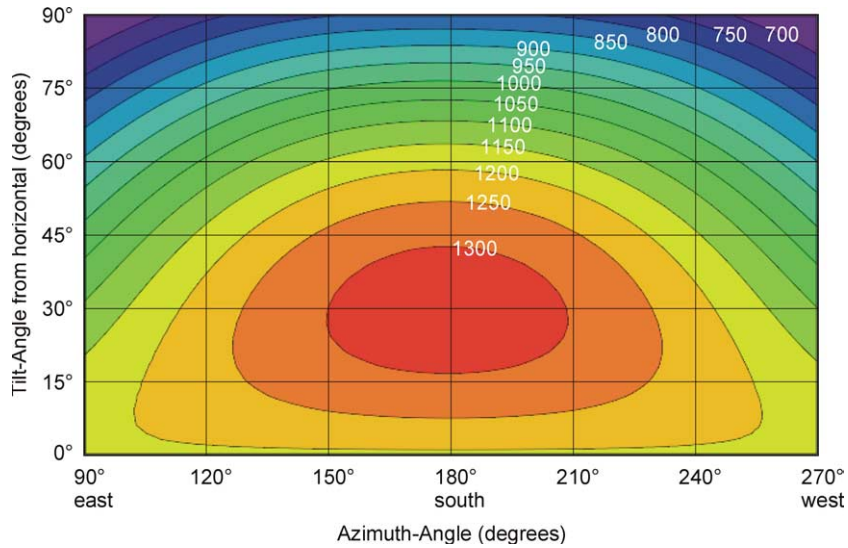


Fig. 10. Total annual incoming solar radiation (in kW h/m²) at the Freiburg site.

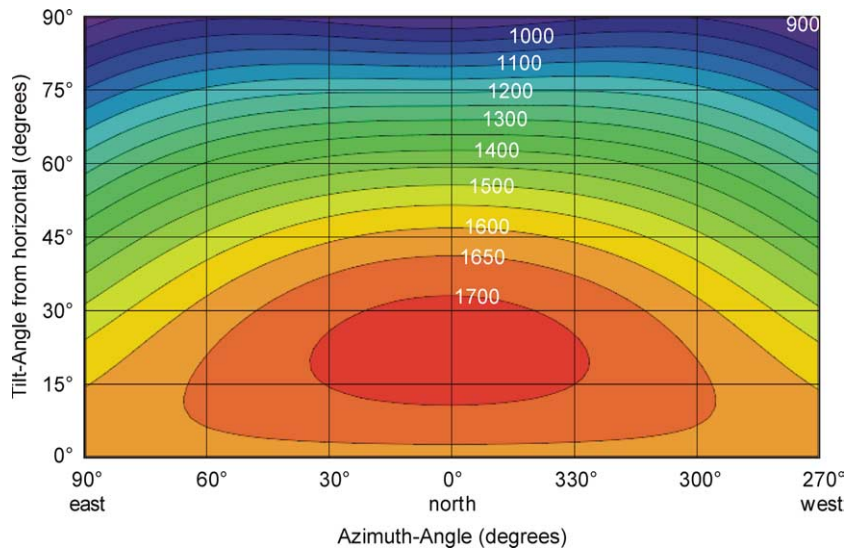


Fig. 11. Total annual incoming solar radiation (in kW h/m²) at the Florianopolis site.

radiation resource in kW h/m² as a function of surface tilt and orientation. Especially for building-integrated photovoltaic (BIPV) installations it is usually argued that sites at higher latitudes are more favorable for vertical facades because the sun is usually lower in the sky. These figures reveal that even at vertical tilt the Florianopolis site (latitude = 27°S) is still receiving a considerable amount of solar radiation, some 10% higher than at the 48°N latitude site Freiburg. As far as surface orientation is concerned, the figures also reveal

that the lower latitude site is less sensitive to azimuth deviations. Figs. 12 and 13 show the total annual DC energy yield, in kW h/kWp per year, respectively, for Freiburg and Florianopolis, using the measured irradiation data and the two-diode model and taking into account temperature effects on crystalline silicon PV device performance. The same surface tilt and orientation effects described in Figs. 10 and 11 can be seen here, with the Florianopolis site showing a smaller sensitivity to azimuth deviations.

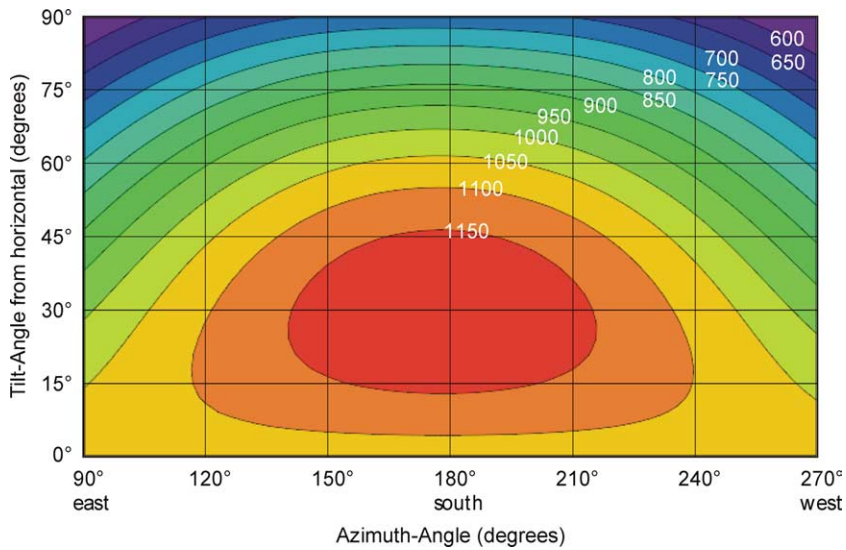


Fig. 12. Total annual DC energy yield (in kW h/kWp) of crystalline silicon PV calculated for the Freiburg site using measured solar radiation data and temperature effects in the two-diode model.

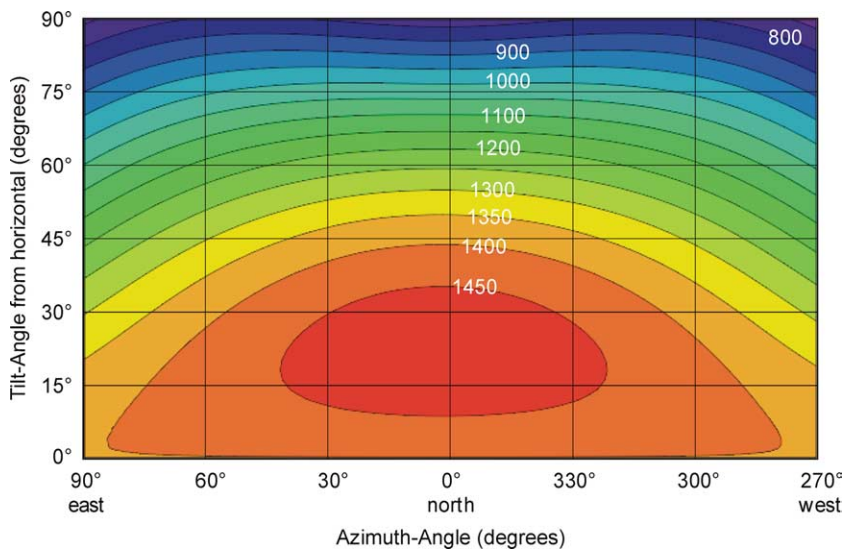


Fig. 13. Total annual DC energy yield (in kW h/kWp) of crystalline silicon PV calculated for the Florianopolis site using measured solar radiation data and temperature effects in the two-diode model.

5. Inverter sizing vs. solar radiation data sampling rates

The calculation of the optimum ratio between the solar array nominal power and the inverter nominal power is fundamental for the correct design of PV plants. As previously shown, the use of hourly averages of solar radiation data leads to considerable differences in the assessment of the solar energy distribution profiles, especially at high irradiation lev-

els. This artifact has consequences in the optimum sizing of inverters.

Figs. 14 and 15 show the optimum relation between the PV array DC nominal power and the inverter nominal AC power ($P_{PV}/P_{Inv,AC,nom}$) for Freiburg as a function of PV array’s surface tilt and azimuth. Calculations are based on mean hourly irradiation values and instant (10 s) irradiation values, respectively. It has been assumed, that 0.5% losses due to inverter power limitation are allowable.

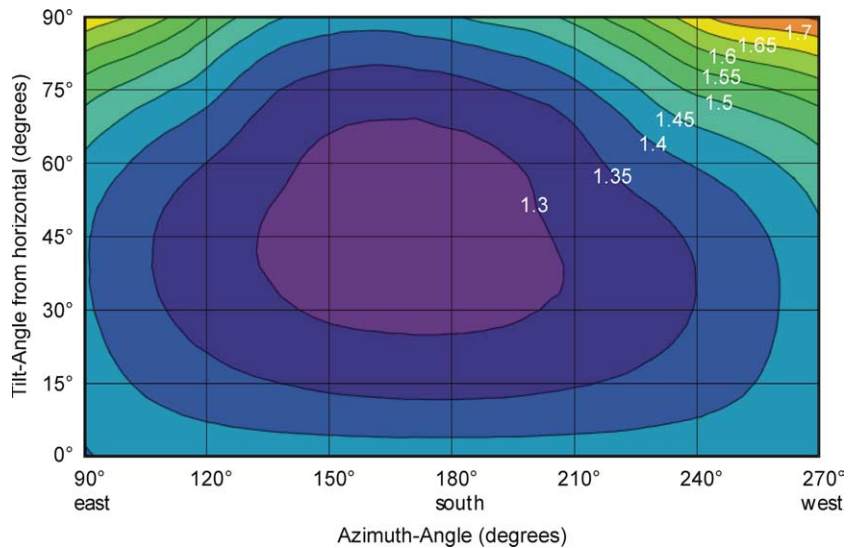


Fig. 14. Optimum relation between a solar PV array DC nominal power (P_{PV}) and an inverter's AC capacity ($P_{Inv,AC,nom}$), calculated for 0.5% losses due to inverter power limitation for the Freiburg site when using mean hourly values of solar radiation data.

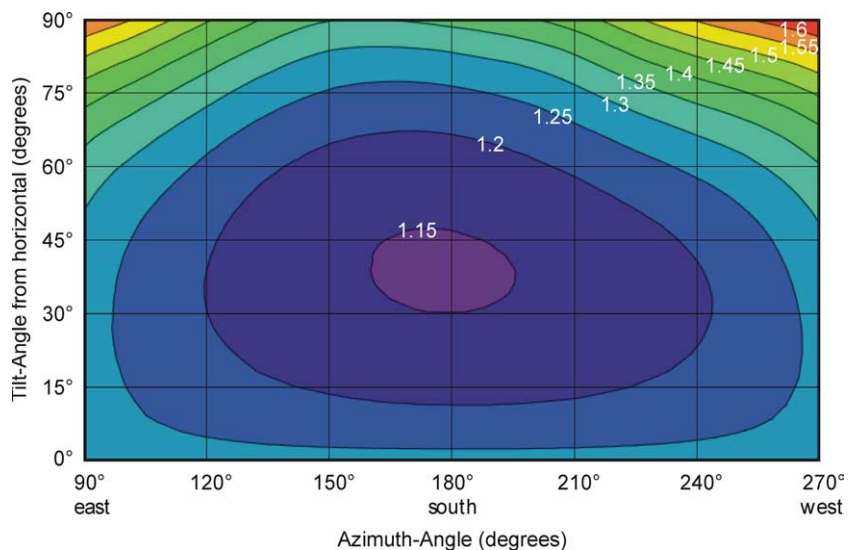


Fig. 15. Optimum relation between a solar PV array DC nominal power (P_{PV}) and an inverter's AC capacity ($P_{Inv,AC,nom}$), calculated for 0.5% losses due to inverter power limitation for the Freiburg site when using instant (10 s) values of solar radiation data.

These figures demonstrate how the use of hourly averages leads to undersizing of the inverters with respect to the PV array nominal power. Instant values also show a smaller tolerance in surface tilt and orientation permissible for the lowest $P_{PV}/P_{Inv,AC,nom}$ relation. This effect can be ascribed to the effect of higher irradiation maxima that occur at more favorable tilts and orientations, which are only detected at higher solar radiation data sampling rates. The slight east bias of the optima can be

assigned to temperature effects impairing the performance of crystalline silicon PV devices more in the afternoon than in the morning. Since higher operating temperatures in the afternoon (west orientation) will lead to a lower PV device performance, a higher $P_{PV}/P_{Inv,AC,nom}$ is allowable.

Figs. 16 and 17 show the optimum relation between the PV array DC nominal power and the inverter nominal AC power ($P_{PV}/P_{Inv,AC,nom}$) for Florianopolis as a function of the PV array's surface

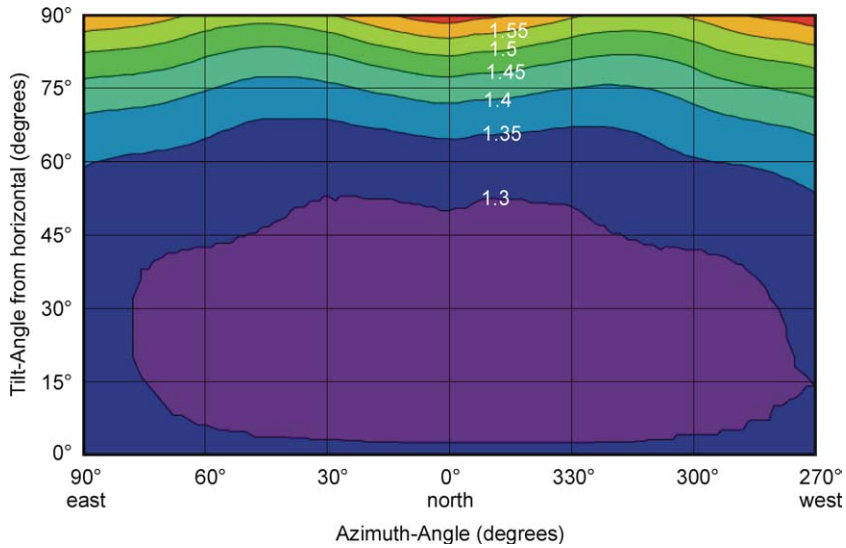


Fig. 16. Optimum relation between a solar PV array DC nominal power (P_{PV}) and an inverter’s AC capacity ($P_{Inv,AC,nom}$), calculated for 0.5% losses due to inverter power limitation for the Florianopolis site when using mean hourly values of solar radiation data.

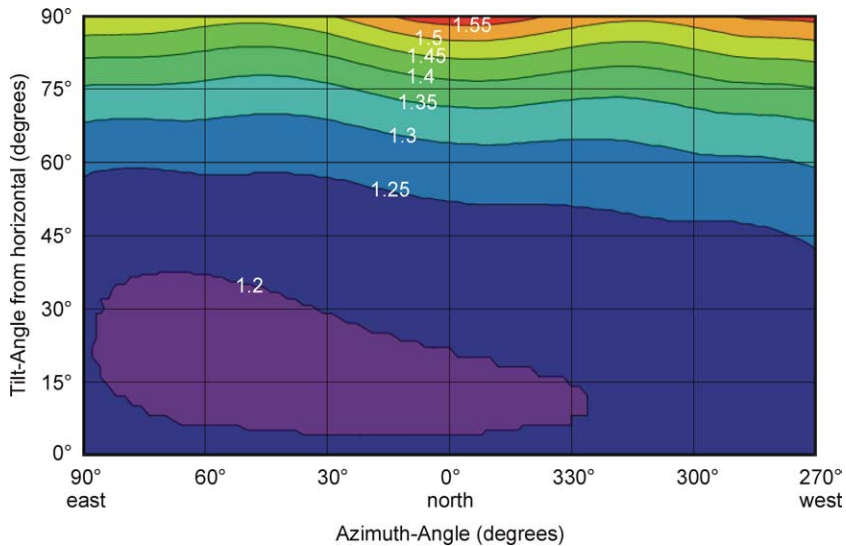


Fig. 17. Optimum relation between a solar PV array DC nominal power (P_{PV}) and an inverter’s AC capacity ($P_{Inv,AC,nom}$), calculated for 0.5% losses due to inverter power limitation for the Florianopolis site when using mean minute values of solar radiation data.

tilt and azimuth. Calculations are based on mean hourly irradiation values and mean minute irradiation values, respectively. 0.5% losses due to inverter power limitation have been allowed. Here again the use of hourly averages leads to undersizing of the inverters with respect to the PV array nominal power. Hourly averages artificially admit a larger tolerance in the PV array’s surface tilt and orientation because the higher energy content of the solar

radiation resource available at high irradiation levels is smoothed when averaged over a 1-h period. When looking at 1-min resolution, a smaller ratio $P_{PV}/P_{Inv,AC,nom}$ is optimum which is also shifted to the east (morning sun), evidencing the strong negative role of the higher PV module temperatures prevailing in the afternoon. A more detailed analysis of the Florianopolis data also reveals some 5% more energy content in the morning than in the

afternoon for the particular year analyzed, which also contributed to the asymmetry seen in Fig. 17.

6. Conclusions

Using different time resolutions for solar radiation data from Freiburg, Germany and Florianopolis, Brazil, we have shown the effects of using averaged data on the optimum inverter sizing for grid-connected photovoltaic systems with crystalline silicon modules.

When calculating the yearly efficiency and losses of inverters due to power limitation, using hourly and 1-min averages, we have demonstrated that actual losses due to inverter undersizing increase with increased averaging time. This reveals that particularly hourly averages hide important irradiation peaks that need to be considered.

Furthermore our results demonstrate that the effect of PV array tilt and orientation on the relation between PV array nominal power and inverter nominal power varies with the time resolution of the solar radiation data. Real conditions are more sensitive to tilt and azimuth than it would be expected from calculations with hourly averages.

In addition, it has been shown from measured STC power of 150 new crystalline PV modules that real module power is still $\approx 3\%$ below nameplate rating. This aspect, together with the fact that in general the yield of PV systems decreases with age, should be taken into account when sizing inverters for grid-connected PV systems.

Acknowledgments

We acknowledge Klaus Kiefer (ISE) for access to the data concerning the STC measurements of 150 new PV modules. R. R  ther wishes to thank the Alexander von Humboldt-Stiftung for partial sponsorship of a sabbatical period at ISE in June/July 2004 and Dr. Tim Meyer (ISE) for hosting this sabbatical and for the valuable comments and suggestions to this manuscript.

References

Baumgartner, F.P., Scholz, H., Brey, A., Roth, S., 2004. MPP voltage monitoring to optimise grid connected system design rules. In: Proceedings of the 19th European Photovoltaic Solar Energy Conference, Paris, France.

H  berlin, H., Borgna, L., K  mpfer, M., Zwahlen, U., 2005. Total Efficiency η -tot—A new quantity for better characterisation of grid-connected PV inverters. In: Proceedings of the 20th

European Photovoltaic Solar Energy Conference, Barcelona, Spain.

Hecktheuer, L.A., Krenzinger, A., Prieb, C.W.M., 2001. Rated versus measured power of PV modules used in Brazilian rural properties electrification. In: Proceedings of the 17th European Photovoltaic Solar Energy Conference, Munich, Germany, pp. 800–803.

Jantsch, M., 1996. Systemtechnische Untersuchung des Nutzungsgrades photovoltaischer Anlagen—Analyse und Optimierung von Strukturen und Wirkungszusammenh  ngen. Ph.D. Thesis, Fakult  t f  r Elektrotechnik—Universit  t Fredericiana Karlsruhe, ISBN 3-18-333606-5, VDI Verlag GmbH, D  sseldorf, Germany, pp. 1–124.

Keller, L., Affolter, P., 1995. Optimizing the panel area of photovoltaic system in relation to the static inverter. *Solar Energy* 55, 1–7.

Kiefer, K., 2004. Fraunhofer ISE Annual Report.

Perezagua, E., Demarcq, F., Alferov, Z.I., Bal, J.-L., de Segundo, K., Dimmler, B., Goetzberger, A., Beunza, C.I., Lojkowski, W., Nowak, S., Sinke, W., van der Vleuten, P., van Zolingen, R., 2004. A vision for photovoltaic technology for 2030 and beyond. In: Preliminary report by the Photovoltaic Technology Research Advisory Council (PV-TRAC), Presented at the Conference “Future Vision for PV: A Vision for PV Technology for 2030 and Beyond”, Brussels, Belgium, pp. 1–40.

Photon International—The Photovoltaic Magazine, 2004. Annual PV module survey, March 2004.

Pregelj, A., Begovic, M., Rohatgi, A., 2002. Impact of inverter configuration on PV system reliability and energy production. In: Proceedings of the 29th IEEE Photovoltaic Specialists Conference, New Orleans, USA, pp. 1388–1391.

R  ther, R., Dacoregio, M.M., 2000. Performance assessment of a 2 kWp grid-connected, building-integrated, amorphous silicon photovoltaic installation in Brazil. *Prog. Photovolt. Res. Appl.* 8, 257–266.

R  ther, R., Mani, G.T., del Cueto, J., Adelstein, J., Montenegro, A., von Roedern, B., 2003. Performance test of amorphous silicon modules in different climates: higher minimum operating temperatures lead to higher performance levels. In: Proceedings of the 3rd World Conference on Photovoltaic Energy Conversion, Osaka, Japan, pp. 501–504.

R  ther, R., Beyer, H.G., Montenegro, A.A., Dacoregio, M.M., Salamoni, I.T., Knob, P., 2004. Performance results of the first grid-connected, thin-film PV installation in Brazil: temperature behaviour and performance ratios over six years of continuous operation. In: Proceedings of the 19th European Photovoltaic Solar Energy Conference, Paris, France, pp. 3091–3094.

Shima, M., Isomura, M., Wakisaka, K., Murata, K., Tanaka, M., 2005. The influence of operation temperature on the output properties of amorphous silicon-related solar cells. *Sol. Energy Mater. and Solar Cells* 85, 167–175.

Sunways, 2004. Sunways NT 6000 Inverter. Available from: <www.sunways.de/em/products/solarinverter/technicalDetails.php>.

van der Borg, N.J.C.M., Burgers, A.R., 2003. Inverter undersizing in PV systems. In: Proceedings of the 3rd World Conference on Photovoltaic Solar Energy Conversion, Osaka, Japan, pp. 517–520.

Woyte, A., Islam, S., Belmans, R., Nijs, J., 2003. Undersizing the inverter for grid-connection—where is the optimum? In:

- Proceedings of the 18th Symposium Photovoltaische Solar-energie, Bad Staffelstein, Germany, pp. 414–419.
- Würth Solergy, 2003. Fitting and operating instructions—low voltage grid inverter solarStar 1200. Available from: <www.wuerth-elektronik.de>.
- Zilles, R., Oliveira, S.H.F., 2001. 6.3 kWp photovoltaic building integration at Sao Paulo University. In: Proceedings of the 17th European Photovoltaic Solar Energy Conference, Munich, Germany, pp. 1975–1978.
- Zilles, R., Ribeiro, C., Moszkowicz, M., 1998. Power rating and the need of photovoltaic modules measurements in Brazilian dissemination program. In: Proceedings of the 2nd World Conference on Photovoltaic Energy Conversion, Vienna, Austria, pp. 2009–2012.